JOURNAL OF CATALYSIS 102, 180–189 (1986)

The Influence of Acid Site Distribution on the Catalytic Deactivation of Sulfonated Poly(styrene-divinylbenzene) Membrane Catalyst

Y. C. CHEE AND S. K. IHM[1]

Department of Chemical Engineering, Korea Advanced Institute of Science and Technology, Seoul 131, Korea

Received March 16, 1986; revised June 17, 1986

The influence of the acid site distribution on the catalytic deactivation of sulfonated poly(styrene-divinylbenzene) membranes in ethanol dehydration was investigated with a differential flow reactor operated at 120°C and 1 atm. Two kinds of the membrane catalysts with the same ion-exchange capacity prepared by different sulfonation methods showed very different deactivation dynamics. The deactivation behaviors were explained through a Langmuir–Hinshelwood kinetics combined with the inhibition due to product water by assuming the different initial distributions of the acid site inside the gelular microparticle. © 1986 Academic Press, Inc.

INTRODUCTION

Macroporous resins consist of agglomerates of the polymer gel microparticles interspersed with macropores (*1*). Much research has been made on the kinetics of alcohol dehydration and esterification with gelular (*2–4*) or with macroporous (*5, 6*) resins.

Klein *et al.* (*7*) demonstrated that nonuniform distribution of the sulfonic acid groups could be obtained by sulfonating poly(styrene-divinylbenzene) resins incompletely and that the distribution of the sulfonic acid groups affects the desulfonation rate of the resins.

In the present study, the influence of the distribution of the sulfonic acid groups within the microparticle is investigated on the deactivation behavior of the macroporous sulfonic acid resin catalyst for the gas phase ethanol dehydration. Ethanol is a small and polar molecule and is expected to swell the polymer effectively, possibly allowing catalysis to occur in the absence of the significant intraparticle concentration gradients (*3, 6*). The intrinsic reaction kinetics for the system had been well established by other investigators (*2, 8–10*). Water, one of the products of the dehydration, can deactivate the catalysts by inhibiting the reaction (*3*) or by desulfonation above 100°C (*7, 11*).

Two membrane type catalysts of the macroporous poly(styrene-divinylbenzene) resins were prepared. The polymer membranes with the same physical properties had been sulfonated in two different ways, resulting in the same overall ion-exchange capacity (1.0 meq H^+/g cat).

The catalytic reaction conditions were chosen similar to those of Kabel and Johanson (*2*). The deactivation pattern of the dehydration reaction was explained in terms of the difference in the sulfonic acid group distribution within the microparticle.

Four different models on the initial acid site distribution were compared to see how they can result in the different deactivation behavior when the same Langmuir–Hinshelwood kinetic expression and water inhibition are introduced for the diffusion limiting microparticle.

EXPERIMENTAL

Membrane preparation. Macroporous poly(styrene-divinylbenzene) membranes were prepared from styrene (Aldrich, 99%),

[1] To whom all correspondence should be addressed.

0021-9517/86 $3.00

TABLE 1

Composition of the Monomers

Component	wt%
Styrene	44.05
Divinylbenzene	13.79
Ethylstyrene	11.36
t-Amyl alcohol	15.68
Polybutadiene	14.92
Benzoyl peroxide	0.2

divinylbenzene (Tokyo Kasei, 55% *m*- and *p*- isomer), and t-amyl alcohol (Tokyo Kasei, 99%). Benzoyl peroxide (Hayashi Pure Chem.) and polybutadiene (Aldrich, 45% vinyl, 55% *cis*- and *trans*-1,4,$\overline{M_n}$ 4,500) were used as the initiator and the plasticizer, respectively. Polypropylene gauze (Tokuyama Soda Co.) was used as the support material. The composition of the monomers for the membranes are listed in Table 1. The membranes were synthesized between the two glass plates submerged vertically in a water bath. Temperature of the water bath was held at 50°C for 72 h then at 85°C for 72 h (*12, 13*). Synthesized membranes were washed with distilled water and methanol repeatedly and dried at 80°C under a vacuum of 10^{-3} Torr for 48 h.

Sulfonation. The membranes were chopped into small patches of 1 × 3 mm and sulfonated by two different methods.

Sample I: 0.1 g of the membranes were swollen with 100 ml of nitrobenzene (Hayashi Pure Chem., 99%) at 25°C in a 500-ml Erlenmeyer flask. After 24 h the membranes were transferred into a 1000-ml three-neck round-bottom flask, equipped with a reflux condenser, containing 500 ml of H_2SO_4 (Junsei Chem., 99.6%) at 85°C.

Sample II: 25 ml of H_2SO_4, 32 ml of CH_2Cl_2 (Rots Chem., N.V., 99.5%) and 92 ml of CH_3NO_2 (Hayashi Pure Chem., E.P.) were mixed and stirred vigorously in a 250-ml round-bottom flask at 25°C. Finally, 0.1 g of the membranes was added to the mixture.

Sulfonated membranes were washed with methanol and distilled water until the pH and the color of the effluents did not change any further. Washed membranes were dried at 80°C under a vacuum of 10^{-3} Torr for 48 h and stored under Ar atmosphere.

Characterization. The thickness of the membranes was 0.19 ± 0.01 mm (Fig. 1). The macroporous structure of the membranes were confirmed by the scanning electromicroscopy as shown in Fig. 2. The pore size distributions were obtained by the BET and mercury intrusion method and shown in Fig. 3. The ion-exchange capacities of the sulfonated membranes, titrated with 10% NaOH solution, charged with the sulfonation time as shown in Fig. 4. Two kinds of catalysts with the same total ion-exchange capacity (1.0 meq H^+/g cat) were prepared through their respective sulfonation methods by controlling the sulfonation

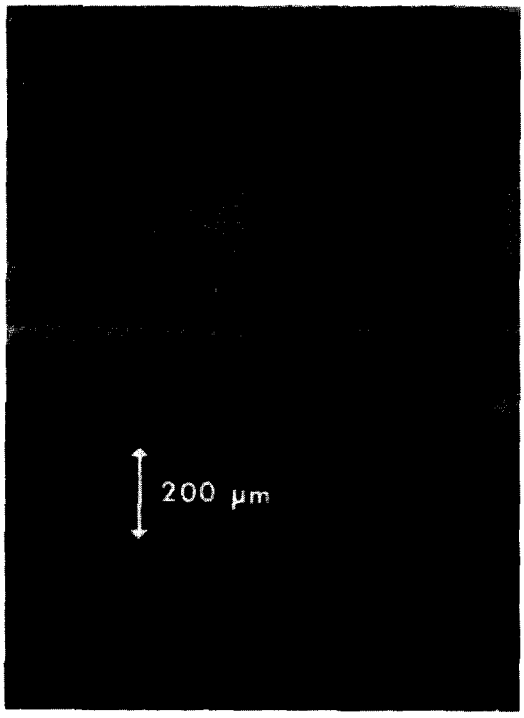

FIG. 1. Cross-sectional view of the membrane (×65).

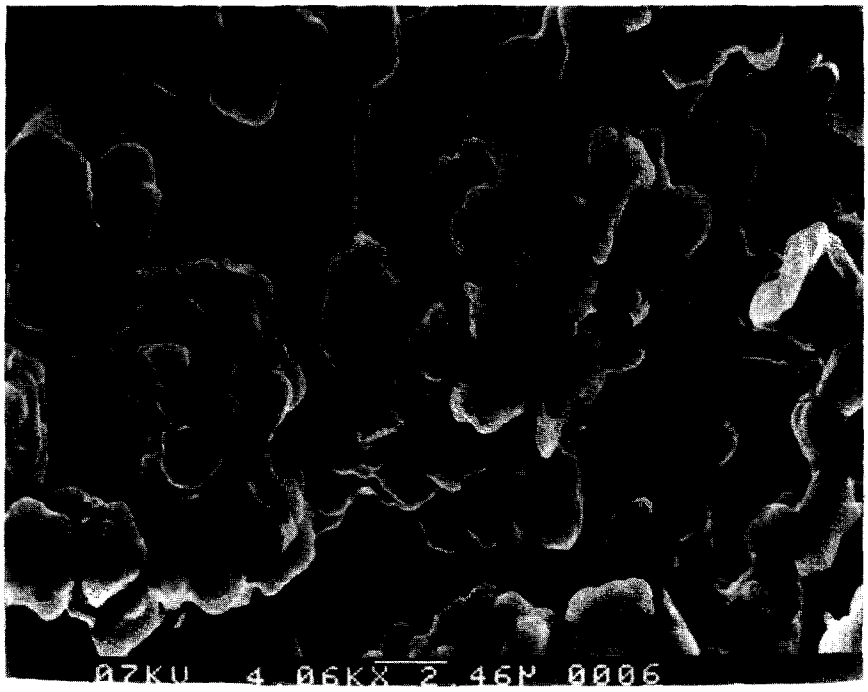

FIG. 2. SEM photograph of the inner structure of the membrane (×4060).

period; i.e., 10 min for sample I and 20 h for sample II.

Ethanol dehydration. The catalytic reactions were carried out in a minireactor shown in Fig. 5. The reactor and evaporator were made of stainless-steel tube with dimensions of 1.25 cm i.d. and 25 cm long and 2.5 cm i.d. and 10 cm long, respectively. Temperature of the system was con-

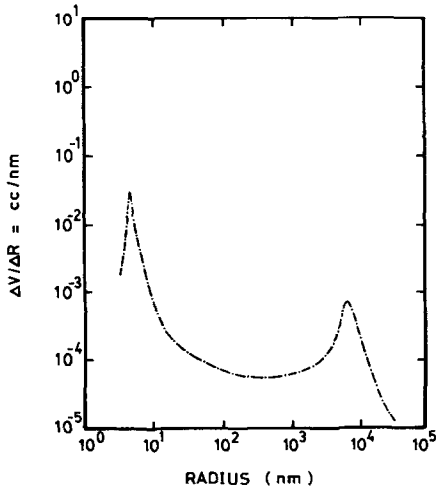

FIG. 3. Pore size distribution of the membrane.

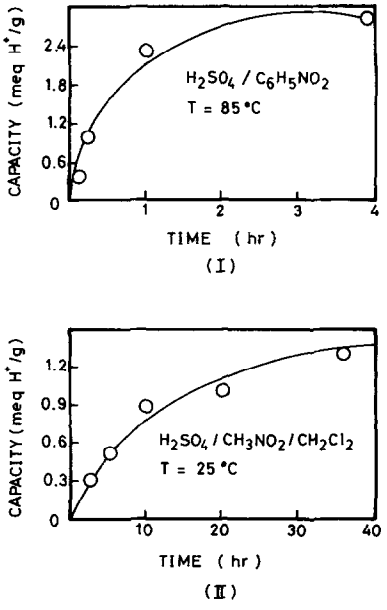

FIG. 4. Ion-exchange capacity vs sulfonation time.

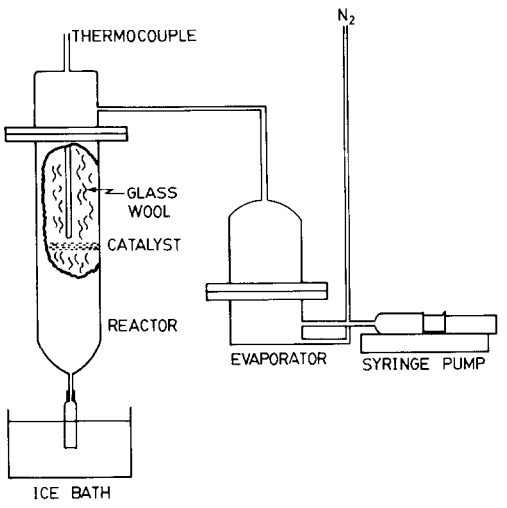

FIG. 5. Reaction apparatus.

trolled within ±0.5°C by wrapping the whole system with the electrical heating tape. Measured amount (0.1 g) of the catalyst prepared by one of the previous methods was loaded in the reactor. The system was purged with nitrogen (99.99%) at 120°C for 30 min before the reaction was started. After N_2 flow was stopped the reactor outlet was connected to the product collector bottle which was submerged in an ice bath. Then only ethanol (Merck, Absolute) was introduced into the evaporator by a syringe pump at a rate of 0.02 ml/min. Temperature of the catalyst bed was 120°C. All of the outlets from the reactor were condensed and collected for 15 min in a 2-ml test tube submerged in an ice bath.

The reaction products were analyzed by gas chromatography with a thermal conductivity cell detector, together with the column packed with Carbowax 20 M (14%) on Chromosorb W (50/60 mesh).

THEORY

Intrinsic kinetics. When ethanol dehydration is catalyzed by sulfonic acid resins, the most probable rate-determining step is reaction between two ethanol molecules adsorbed adjacently (*2, 8–10*). The intrinsic reaction rate equation suggested by Kabel and Johanson (*2*) is given by

$$\bar{r}' = [k_s SLK_A^2/2][P_A^2 - P_E P_W/K_{eq}]/[1 + K_A P_A + K_E P_E + K_W P_W]^2 \quad (1)$$

where $k_s SL/2$ is the reaction rate constant in terms of the moles of alcohol reacted per unit mass of catalyst per unit of time.

According to Gates *et al.* (*14*) and Jerábek *et al.* (*15*), the reaction rate constant per unit mass of catalyst has a power dependence on the concentration level in the unit of equivalent per unit mass of catalyst, i.e.,

$$k' = k'_o[C'/C'_{max}]^m \quad (2)$$

where C'_{max} and k'_o is the capacity and the reaction rate constant per unit mass of fully sulfonated catalyst. Such a dependence was reported for the dehydration of t-butanol (*15*) and also for ethanol and methanol (*3*). If the distribution of sulfonic acid groups of the catalyst were assumed to be uniform, the reaction rate constant per equivalent of sulfonic acid group can be derived from Eq. (2).

$$k'_e = k'/C' = [k'_o/C'_{max}][C'/C'_{max}]^{m-1} = k'_{oe}[C'/C'_{max}]^{m-1}. \quad (3)$$

For ethanol dehydration at 119.3°C, the power m in Eq. (3) was reported by Gates and Johanson (*3*) to increase with the acid site concentration. Based on their result (Fig. 9 of Ref. (*3*)) we assumed the power to increase from $m - 1$ to m when the acid site concentration is higher than a critical concentration C'_c. Equation (3) may be modified as follows depending on the concentration level:

$$k'_e = k'_{oe}[C'_c/C'_{max}]^{m-1}[C'/C'_c]^{m-2} \quad C' \le C'_c \quad (4a)$$

$$k'_{oe}[C'/C'_{max}]^{m-1} \quad C' > C'_c \quad (4b)$$

where k'_{oe} is the rate constant per equivalent sulfonic acid group of the fully sulfonated catalyst. Within the limitations of the information, k_s^*/L by Kabel and Johanson

(2) is equivalent to k'_{oe} because the catalysts were almost fully sulfonated.

Deactivation. When ethanol dehydration is catalyzed by the sulfonic acid resins, product water would inhibit the reaction as shown in Eq. (1). If the amount of water produced is larger than the amount diffused out, the reactivity of the catalyst will decrease with time. Gates and Johanson (*3*) reported that the decrease in the reaction rate was observed for increasing conversions as the product water inhibit the reaction. It is known that when water occupies the sulfonic acid groups in the sulfonated resins two molecules of water are bridged between two sulfonic acid groups (*16*). On the other hand, Klein *et al.* (*7*) reported that water reacts with the sulfonic acid groups and eliminates them from aryl groups of the catalyst above 100°C, and that the desulfonation rate depends on the second order of the sulfonic acid group concentration (*7, 11*).

In this work it was assumed that a part of the water produced, which does not diffuse out but remains in the catalyst, either occupies the sulfonic acid groups or participates in eliminating the acid groups. In both cases a second order dependence of the decreasing rate of the free active sites on the sulfonic acid group concentration is expected because $C' = C_w$ (*11, 16*), i.e.,

$$-\frac{dC'}{dt} = k_d C' C_w = k_d C'^2. \qquad (5)$$

Acid site distribution. Since the aforementioned relationships of kinetics and deactivation rate are intrinsic values obtained from data for the sulfonic acid resin catalysts with a uniform acid site distribution, they can be applied to nonuniformly sulfonated catalysts with the local values of the parameters if they were substituted with the proper local values depending on the radial position.

$$\bar{r}'_A(r) = [k'_e(r)C'(r)K_A^2][P_A^2(r) - P_E(r)P_W(r)/K_{eq}]/[1 + K_A P_A(r) + K_E P_E(r) + K_W P_W(r)]^2 \qquad (6)$$

$$k'_c(r) = k'_{oe}[C'_c/C'_{max}]^{m-1}[C'(r)/C'_c]^{m-2} \quad C'(r) \le C'_c \qquad (7a)$$

$$k'_{oe}[C'(r)/C'_{max}]^{m-1} \quad C'(r) > C'_c \qquad (7b)$$

$$-\frac{dC'(r)}{dt} = k_d C'(r)^2. \qquad (8)$$

Four types of simple acid group distributions were chosen as shown in Fig. 6. The local values of the acid group concentration and the partial pressure of each component in the four distributions can be expressed as follows.

The local acid site concentrations of the catalyst are given:

$$\text{(A)}\quad C'(r) = \text{constant} \qquad 0 \le r \le R_\mu \qquad (9a)$$

$$\text{(B)}\quad C'(r) = B' - D'r \qquad 0 \le r \le R_\mu \qquad (9b)$$

$$\text{(C)}\quad C'(r) = \begin{cases} C'_{max} & r_c \le r \le R_\mu \\ 0 & 0 \le r \le r_c \end{cases} \qquad (9c)$$

$$\text{(D)}\quad C'(r) = E'r \qquad 0 \le r \le R_\mu \qquad (9d)$$

where r is the distance from the center of the microparticle, as shown in Fig. 7. The critical radius r_c in Eq. (9c), within which the sulfonic acid groups are absent, and the constants for Eqs. (9b) and (d) were obtained from the relationship between the lo-

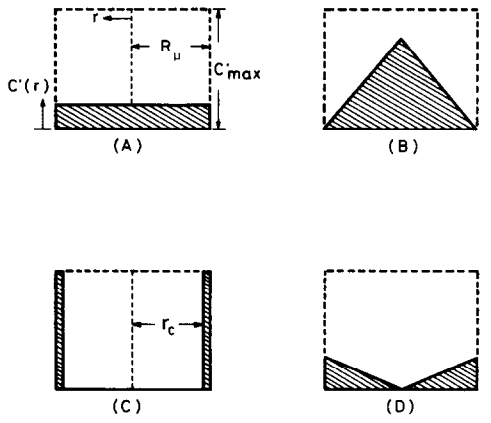

FIG. 6. Schematic diagram of acid site distributions in the microparticle (The overall distribution is assumed uniform over the porous resin catalyst; the shadowed area indicates the local distribution of sulfonic groups.)

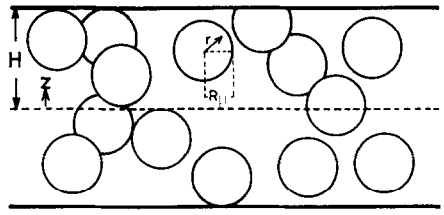

FIG. 7. Schematic diagram of the membrane catalyst.

TABLE 2a

Constants for Eqs. (9)–(20)

C'_{max}	5.2[a]
ε_a	0.7[b]
ρ	1.0[a]
ρ'	0.3[b]

[a] Assumed.
[b] Measured.

TABLE 2b

Constants from Eqs. (9)–(12)

β	$0.93\ R_\mu$
B'	4.0
D'	$4.0/R_\mu$
E'	$1.33/R_\mu$

cal concentration and the total amount of the acid group in the catalyst.

It is assumed that the population of the microparticles is constant throughout the membrane and that the total capacity per microparticle is also constant.

$$C'_{ov} = \int_0^H (1 - \varepsilon_a)\rho e' dz / H\rho' = (1 - \varepsilon_a)(\rho/\rho') \int_0^1 e' dx \qquad (10)$$

where

$$e' = \int_0^{R_\mu} 4\pi r^2 C'(r)\rho dr / \tfrac{4}{3}\pi R^3 \rho = 3 \int_0^1 y^2 C'(y) dy. \qquad (11)$$

By substituting the $C'(r)$s in Eq. (9) and the constants in Table 2a into Eq. (10) one can find that

$$C'_{ov} \simeq (1 - \varepsilon_a)(\rho/\rho')e'. \qquad (12)$$

The critical radius and constants obtained from above are listed in Table 2b.

The interparticle mass transfer and the diffusional limitation in the macropore were found negligible within our experimental range. It can be assumed that the microparticle is in a quasisteady state and that the transient behavior is represented by Eq. (8) only. The microparticle activity can be analyzed by solving the proper differential equations for diffusion and reaction as follows.

$$\frac{D_{ei}}{RT}\left(\frac{\partial^2 P_i(r)}{\partial r^2} + \frac{2}{r}\frac{\partial P_i(r)}{\partial r}\right) - \bar{r}'_i(r) = 0 \quad (i = \text{A, E, and W}) \qquad (13)$$

where

$$\bar{r}'_E(r) = \tfrac{1}{2}\bar{r}'_A(r) \qquad (14)$$

$$\bar{r}'_W(r) = \tfrac{1}{2}\bar{r}'_A(r) - k_d C'(r)^2. \qquad (15)$$

Since the reaction was induced at 1 atm and there were no ethanol and water initially the boundary conditions (B.C.) and initial condition (I.C.) are as follows.

$$\text{B.C. } P_A = 1.0 \text{ atm} \quad \text{at } r = R_\mu \qquad (16)$$

$$\frac{\partial P_i}{\partial r} = 0 \ (i = \text{A, E, and W}) \quad \text{at } r = 0 \qquad (17)$$

$$\text{I.C. } P_E, P_W = 0 \quad \text{at } t = 0,\ 0 \le r \le R_\mu \qquad (18)$$

$$D_{eA} \simeq D_{eE} \simeq D_{eW} = 1.0 \times 10^{-3} \text{ cm}^2/\text{sec}. \qquad (19)$$

The reaction rate constant and equilibrium adsorption constants for Eq. (14) and Eq. (15) were adopted from Kabel and Johanson (*2*) and listed in Table 3.

Reaction rate. The reaction rate at each position of the catalyst was calculated from Eq. (6) using local values of the acid site concentration, $C'(r)$ in Eq. (9), reaction rate constant, $k'_e(r)$ in Eq. (7), and partial pressure of each components obtained from Eqs. (13)–(19). The overall reaction rate

TABLE 3

Constants for Kinetics and Adsorption

T, °C	K_A	K_W	K_E	K_{eq}	$k'_{oe}(=k^*/L) \times 10^2$
120.0	3.4	7.0	(0)	25.2	4.4

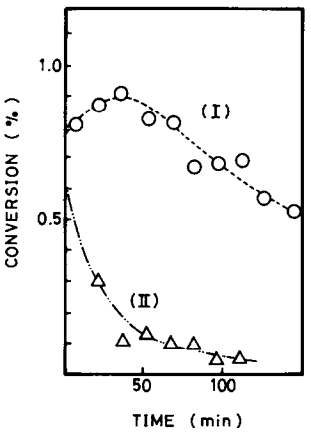

FIG. 8. Empirical result of ethanol conversion with the time (○, catalyst I; △, catalyst II).

per gram of catalyst was calculated from the local reaction rate as

$$\bar{R}'_A = 3(1 - \varepsilon_a)(\rho/\rho') \int_0^1 y^2 r'_A(y)dy. \quad (20)$$

By adjusting $k'(r)$ and $C'(r)$ in Eq. (6) with the lapse of the time, respectively, as Eq. (7) and Eq. (8), the reaction rate at each moment was calculated. Conversion was obtained from the reaction rate, amount of catalyst, and reactant feed rate.

RESULTS AND DISCUSSION

Ethanol conversion obtained with the catalyst I and II were shown in Fig. 8. At the beginning of the reaction, the average number of alcohol molecules reacted per equivalent of acid group per minute was about 0.027 (0.8% conversion), about 35% larger than other results (*2, 3*). However, the activity of the catalysts decreased as the reaction proceeded. This decrease in catalytic activity was supposed to be caused by water inhibition because water was not detected in the product and because the reused catalyst, on being flushed with nitrogen at 120°C for 30 min, showed the same initial activities and deactivation. Conversions per equivalent were within the range of the decrease in the reaction rate by water inhibition reported by Gates and Johanson (*3*) (moles of ethanol reacted/equivalents of catalysts-minutes >0.02).

Deactivation patterns of the two catalysts were quite different, implying that the difference in the acid site distribution influenced the deactivation patterns. Catalyst I showed a maximum in conversion after the initial period, which was considered as the representative of the fresh catalyst being swollen by the reactant (*3*). After the maximum, the conversion decreased slowly. On the other hand, the initial deactivation rate of the catalyst II was higher than the catalyst I, which implies that the local concentration of the acid groups in the catalyst II is higher than in the catalyst I. From the sulfonation conditions of the catalysts it can be expected that the acid site distribution in catalyst I, which was sulfonated after preswelling, would be uniform as the type A in Fig. 6. If the sulfonic acid groups on the outer part of the microparticles had been split off during the washing, the acid site distribution in the catalyst I will be the type B. On the other hand, the catalyst II in which the inner gelular phase is becoming accessible only gradually (*7*) will have nonuniform distribution of the acid group as the type C or the type D.

Figures 9a and b are the numerical results of the ethanol conversion for the four types of the distributions calculated with various k_d, m and C'_c values. When there is no deactivation, i.e., $k_d = 0$. the conversions increased with time and approached to the steady state values (Fig. 9a). Activity of the type C was the highest and it did not change with m and C'_c because the local reaction rate constant of it, $k'_{oe}C'_{max}$ according to Eq. (7), is higher than that of the others and it does not change with both of the parameters. The difference in activity between the type C and others are more significant as m is larger than C'_c is smaller.

According to Jeràbek *et al.* (*15*), m is the number of the active sites participating in the rate-determining step of t-butanol dehydration. And it is known that in the ethanol dehydration and rate-determining step oc-

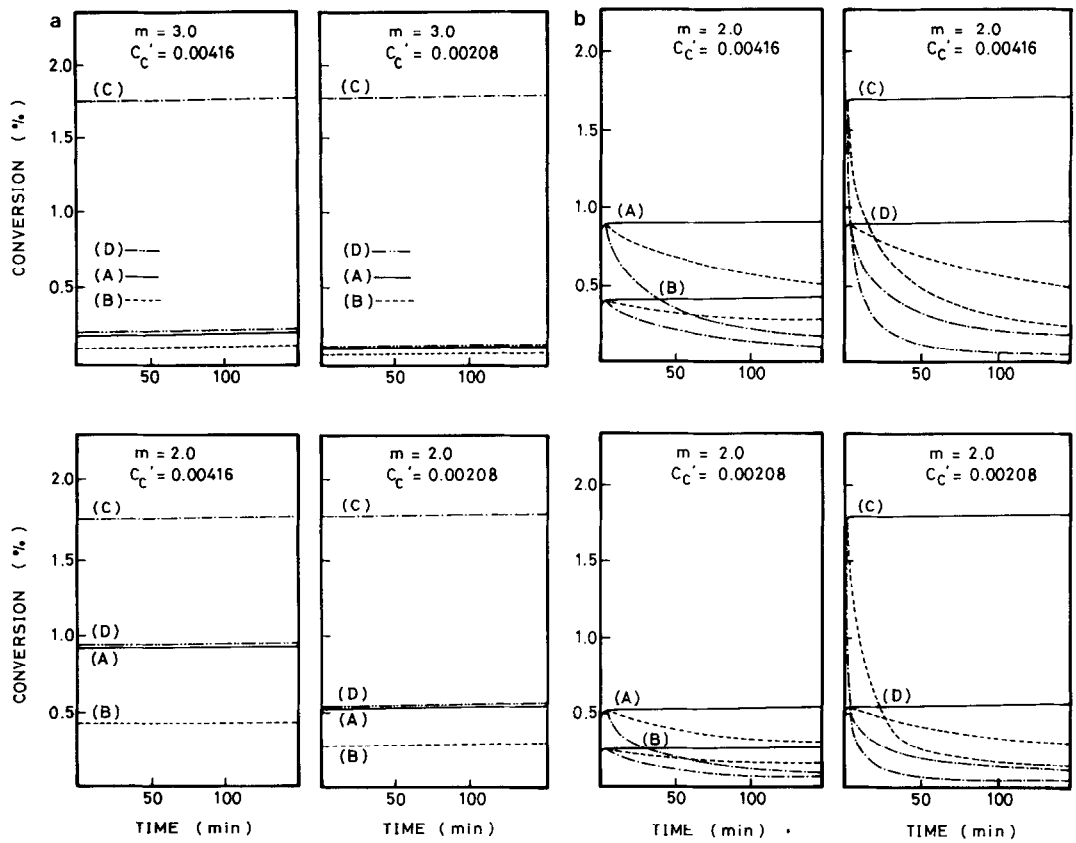

FIG. 9. (a) Numerical result of ethanol conversion with the time (k_d = 0.0). (b) Numerical result of ethanol conversion with the time. (—) k_d = 0.0, (– – –) k_d = 7.0, (– · –) k_d = 40.0.

curs between the two alcohol molecules bound to the adjacent sulfonic acid groups (*3, 4, 17*). On the basis of those results, we assumed m of the ethanol dehydration to be 2. Figure 9b is the result with $m = 2$ and various k_d and C_c'. For $k_d > 0$, the deactivation rate of the type C was faster than the others and after some period the catalytic activity was the lowest. The deactivation patterns and the initial activity of the type A and the type D were very similar, which means that the difference of the acid site distribution between the two types is not sufficient to explain the different deactivation patterns of our experiment. But the deactivation rate of the type D was slightly faster than that of the type A.

By comparing the empirical result of the catalyst I with the numerical results of the type A, B, and D, it was found that the distribution of the type A is more appropriate for the catalyst I than the others. The values of k_d and C_c' were 7.0 (mole/g cat min)$^{-1}$ and 4.16 (meq H^+/g cat), respectively. By the same way, the type C was more appropriate for the catalyst II than the type D. But, the numerical results for the type C, with the same values of k_d and C_c', were higher than the empirical results of the catalyst II.

According to Diemer *et al.* (*6*), the number of ensembles of the hydrogen bonded sulfonic acid groups, which were suggested as the catalytic sites of the dehydration (*3, 17*), on the microparticle surface is about half of that at the interior of the gel phase.

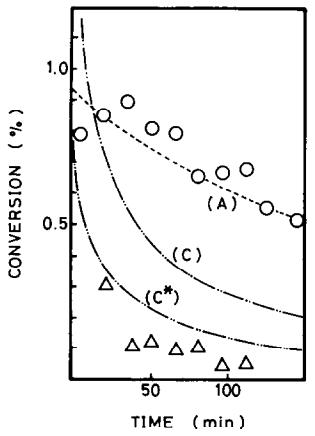

FIG. 10. Comparison of the empirical and the numerical results of ethanol conversion (k_d = 7.0, m = 2.0; ○, catalyst I; △, catalyst II).

This seems to be valid for the catalyst II since most of the sulfonic acid groups are believed to be located on the microparticle surface. If the activity of the catalyst II is taken as half of the internal sulfonic groups, the deactivation pattern becomes closer to the experimental data as shown by the curve C* in Fig. 10. Other reasons such as the decrease in the effective diffusivity induced by additional crosslinking due to local dense sulfonation (*11*) may also reduce the catalytic activity of the catalyst II.

From this work, it is shown that the distribution of sulfonic acid groups within the microparticles of the macroporous sulfonic acid resins can affect the deactivation patterns of the catalyst when they were used in ethanol dehydration at 120°C. Such deactivation patterns can be represented successfully by Langmuir–Hinshelwood type reaction model combined with decrease in the number of the free active sites. The catalyst with uniform and low local acid site concentration showed slow deactivation. On the other hand, the deactivation rate of the catalyst with nonuniform and high local capacity was higher. It is suggested that the lower activity of the latter catalyst is due to acid sites on the microparticle surface being less active than those in the gel-phase interior.

APPENDIX: NOMENCLATURE

B'	constant for Eq. (9b)
C'	sulfonic acid group concentration, g mole/g cat
C'_c	critical concentration of sulfonic acid group, g mole/g cat
C'_{max}	maximum concentration of sulfonic acid group, g mole/g cat
D'	proportional constant for Eq. (9b)
D_{ei}	effective diffusivity of component i, cm^2/sec
E'	proportional constant for Eq. (9d)
H	thickness of the membrane, mm
k'	reaction rate constant, g mole/g cat min
k'_e	reaction rate constant per equivalent of acid group, g mole/equivalent min
k_d	deactivation rate constant (g mole/g cat min^{-1})
k_s	forward specific reaction velocity, min^{-1} (*2*)
k_s^*	$k_sSL/2$ (*2*)
K_{eq}	thermodynamic equilibrium constant, dimensionless
K_i	Langmuir equilibrium adsorption constant of component i, atm^{-1}
L	total adsorption sites on catalyst, g mole/g cat (*2*)
m	power for Eq. (2)
P_i	partial pressure of component i, atm
r	distance from center of the microparticle, mm
r_c	critical distance from center of the microparticle, mm
$\bar{r}'_i$	reaction rate of each component, g mole/g cat min
R	gas constant, cm^3 atm/mole °K
$\bar{R}'_i$	overall reaction rate of each component, g mole/g cat min
R_μ	radius of the microparticle, mm
S	number of catalytic sites adjacent to a given site, dimensionless
t	reaction time, min
T	reaction temperature, °K
x	dimensionless distance from center of the membrane, z/H
y	dimensionless distance from center of the microparticle, r/R_μ

z distance from center of the membrane, mm
β r_c/R_μ
ε_a porosity of the catalyst, dimensionless
ρ density of the microparticle, g/cm^3
ρ' apparent density of the membrane catalyst, g/cm^3

Subscripts

A ethanol
E ethyl ether
W water
ov overall value
o in the fully sulfonated catalyst

REFERENCES

1. Pitochelli, A. R., "Ion-Exchange Catalysis and Matrix Effects." Rohm & Haas, Philadelphia, 1975.
2. Kabel, R. L., and Johanson, L. N., *AIChE J.* **8,** 621 (1962).
3. Gates, B. C., and Johanson, L. N., *J. Catal.* **14,** 69 (1969).
4. Gates, B. C., and Johanson, L. N., *AIChE J.* **17,** 981 (1971).
5. Dooley, K. M., Williams, J. A., Gates, B. C., and Albright, R. L., *J. Catal.* **74,** 361 (1982).
6. Diemer, R. B., Jr., Dooley, K. M., Gates, B. C., and Albright, R. L., *J. Catal.* **74,** 361 (1982).
7. Klein, J., Widdecke, H., and Bothe, N., *Macromol. Chem. Suppl.* **6,** 211 (1984).
8. Lapidus, L., and Peterson, T. I., *AIChE J.* **11,** 891 (1965).
9. Kabel, R. L., *AIChE J.* **14,** 358 (1968).
10. Mezaki, R., and Kittrell, J. R., *AIChE J.* **14,** 513 (1968).
11. Bothe, N., Dosher, F., Klein, J., and Widdecke, H., *Polymer* **20,** 850 (1979).
12. Jeong, J. H., Chee, Y. C., and Ihm, S. K., *Hwahak Konghak* **24**(2), 113 (1986).
13. Minkiewicz, J. V., Milstein, D., Lieto, J., Gates, B. C., and Albright, R. L., *in* "Chemically Modified Surfaces in Catalysis and Electrolysis" (J. S. Miller, Ed.), pp. 9–26. 1982.
14. Gates, G. C., Winouskas, J. S., and Heath, H. W., Jr., *J. Catal.* **24,** 320 (1974).
15. Jeràbek, K., Bazànt, V., Beranek, L., and Setìnek, K., *in* "Proceedings, 5th International Congress on Catalysis, Palm Beach, 1972" (J. W. Hightower, Ed.), pp. 1193–1203. North-Holland, Amsterdam, 1973.
16. Zundel, G., and Metzger, H., *Z. Phys. Chem. (Frankfurt)* **59,** 225 (1968).
17. Thornton, R., and Gates, B. C., *in* "Proceedings, International Congress on Catalysis," Palm Beach, 1972" (J. W. Hightower, Ed.), pp. 357–369. North-Holland, Amsterdam, 1973.